Pergamon

Int. J. Heat Mass Transfer. Vol. 39, No. 7, pp. 1503–1517, 1996

0017–9310/96 $15.00+0.00

0017–9310(95)00229–4

Application of the boundary element method to inverse heat conduction problems

D. LESNIC, L. ELLIOTT and D. B. INGHAM†

Department of Applied Mathematical Studies, University of Leeds, Leeds LS2 9JT, U.K.

(*Received* 10 *October* 1994 *and in final form* 16 *February* 1995)

Abstract—The solution of the one-dimensional, linear, inverse, unsteady heat conduction problem (IHCP) in a slab geometry is analysed. The initial temperature is known, together with a condition on an accessible part of the boundary of the body under investigation. Additional temperature measurements in time are taken with a sensor positioned at an arbitrary location within the solid material, and it is required to determine the temperature and the heat flux on the remaining part of the unspecified boundary. As the problem is improperly posed the direct method of solution cannot be used and hence the least squares, regularization and energy method have been introduced into the boundary element method (BEM) formulation. When noise is present in the measured data some of the numerical results obtained using the least squares method exhibit oscillatory behaviour, but these large oscillations are substantially reduced on the introduction of the minimal energy technique based on minimizing the kinetic energy functional subject to certain constraints. Furthermore, the numerical results obtained using this technique compare well with the results obtained using regularization procedures, showing a good stable estimation of the available test solutions. Further, the constraints, subject to which the minimization is performed, depend on a small parameter of which selection is more natural and easier to implement than the choice of the regularization parameter, which is always a difficult task when using the regularization procedures.

1. INTRODUCTION

Inverse problems arise in many heat transfer situations when experimental difficulties are encountered in measuring or producing the appropriate boundary conditions. A problem that frequently occurs in practice in heat conduction theory consists of estimating the temperature and the heat flux values on the space surface of a conducting solid through the use of experimental measurements taken within or at a secondary space surface of the body, i.e. the inverse heat conduction problem (IHCP), see ref. [1]. Typical practical applications are the estimation of the temperature and the heat flux at the surface of the body under investigation, e.g. re-entry vehicles, combustion chambers, calorimeter-type instrumentation, etc.

Nevertheless the ICHP is more difficult to solve, both analytically and numerically, than a direct problem. In the direct problem the errors arising from boundary value measurements are damped when evaluating the interior temperature because of the diffusive nature of the heat conduction process [2], whilst in inverse problems internal measurement errors are extrapolated and amplified as the unknown boundary values are calculated. Consequently special corrective methods should be employed in order to reduce the effect of error growth and propagation when dealing with inverse problems. In addition, there may be questions of the existence and the uniqueness of the surface condition history, as predicted by discrete and relatively inaccurate internal measurements or modelling errors. The obvious noise, present in any measurement, ensures that any solution obtained is only approximate. Because of these highly sensitive conditions the IHCP is mathematically regarded as an ill-posed problem in the sense as described by Hadamard [3].

In the last 30 years many theoretical studies, e.g. refs. [4–6], have been undertaken for solving the IHCP, providing an insight into the mathematics of the problem although they introduce additional hypotheses which are not, in general, satisfied in practice. Consequently, in practical problems numerical methods appear more useful although they are quite complicated and require modifications and powerful techniques to be applied when dealing with ill-posed problems.

The first step in solving numerically an IHCP is to discretize the solution domain using finite differences or finite elements or, to use boundary discretizations such as boundary elements. The advantage of applying finite differences and finite elements is that in these methods the fully nonlinear heat conduction equation can be discretized, although they usually produce instabilities in the numerical schemes and require a large number of cells or elements. On the other hand, when using the BEM only the boundary needs to be discretized and this gives rise to savings in computation time and storage requirements. In addition, in the BEM no domain discretization is needed and so the location of internal points, where the tem-

† Author to whom correspondence should be addressed.

perature is measured, can be chosen in a quite arbitrary way. Furthermore, unlike other numerical methods, the BEM gives in a straightforward manner both the unknown surface temperature and the heat flux. Although the surface heat flux is more difficult to calculate accurately than the surface temperature, see ref. [7], their direct determination avoids the additional finite differencing required in the conventional finite element approach [8]. It is only in the last few years that the BEM has been considered in the study of IHCP and has been utilized by, for example, refs. [9–12].

After the boundary value problem has been discretized the next step in solving an improperly posed problem is to stabilize the numerical solution. The implementation of the known boundary information, together with the discrete internal measurements, always reduces to finding the solution of an algebraic system of equations, no matter which numerical method is used. At this stage the system of equations is considerably smaller when using the BEM than that generated by an equivalent finite-difference or finite element approximation. Nevertheless, since the problem is not well-posed, a direct method of solution of this system of equations, such as a Gauss elimination procedure (in the linear case), will not be possible or will produce very inaccurate results, and special corrective procedures must be introduced. This inaccuracy is caused by the extreme sensitivity (instability) of the solution to the inaccurate experimental measurements.

To overcome the stability problem, one possible approach is to record the temperature history at more locations than the number of unknowns in the algebraic equations to be solved. Then the system of equations becomes overdetermined and can be solved using a least squares method that minimizes the error between the computed and measured sensor temperatures. As more data are known this will reduce the non-uniqueness caused by random errors, i.e. reduce the space on which solutions are determined independently of the measure (norm) of continuous dependence. However, for multidimensional problems it may not be possible to introduce more sensor measurements because of the large number of elements already required for the discretization. In addition, the method presents inconsistency and for strongly ill-posed problems, such as the backward heat equation, this procedure leads to incorrect results even for free error measured data [13].

A method of dealing with such problems is the regularization technique which modifies the least squares method by adding a regularization coefficient, which multiplies the sum of the squares of the discrete temperatures or heat fluxes or their consecutive differences, as described by Tikhonov and Arsenin [14]. The quasi-inversion method was developed by Weber [15] and it approximates the heat equation by a hyperbolic equation, namely the telegraph equation, for which the problem becomes well-posed. Other methods which have been adopted in the last few years, and are based more or less on the regularization process, are the function specification [16], the minimal energy [17], the least squares adjustment [18], the conjugate gradient with the adjoint equation [19], the mollification [20] and the dynamic programming [21] methods.

In this study the solution of the one-dimensional, unsteady linear heat conduction equation in a slab geometry with constant physical properties is analysed. The IHCP is formulated as follows. The initial temperature distribution is specified, together with a general space boundary condition of the Robin type, which involves a relationship between the temperature and the heat flux. In addition, temperature readings at certain points within the interior domain and at particular times are known. The aim of this paper is to use the BEM and the minimal energy technique to solve this IHCP, namely to determine the temperature and the heat flux on the remaining boundary and using this information, and the given boundary conditions, the temperature throughout the whole domain. The BEM for the numerical solution of this class of improperly posed problems is applied, since this choice of method does not require any domain discretization. This means that the unknowns are calculated only at boundary nodes and at selected internal points. Due to the improper nature of the IHCP, the direct method has been found not to be applicable and therefore the least squares, the regularization and the minimal energy methods have been introduced into the BEM and the results are compared with the analytical solutions over a wide range of test examples. The effects of the location of internal temperature measurements in relation to the distance from the surface where the temperature and the heat flux are unknown are also investigated. For exact data the results for the surface temperature and heat flux obtained using the numerical methods show good agreement with the analytical solution. It is shown how the unknown surface temperature and heat flux can be determined accurately over a large range of the time domain, and by extending the known boundary condition for a suitable additional time, can produce accurate results over the whole of the earlier time domain. However, when noise is present in the data the least squares method produced oscillatory and inaccurate results and in this case these instabilities can be alleviated by using the minimal energy method, which is based on the minimization of the kinetic energy functional subject to certain constraints.

Finally the numerical results for the surface temperature and heat flux obtained using the minimal energy technique compare well with the numerical results obtained using zeroth- or first-order regularization procedures and offer a stable and good approximate estimate of the available analytical solutions.

2. FORMULATION OF THE PROBLEM

The mathematical formulation of the IHCP considered in this study can be described by the following boundary value problem. The governing heat conduction equation in a slab geometry, namely

$$\frac{\partial T(x,t)}{\partial t} = \frac{\partial^2 T(x,t)}{\partial x^2} \quad \text{for } (x,t) \in (0,1) \times (0,\infty) \quad (1)$$

has to be solved subject to the boundary conditions

$$T(x,0) = T_0(x) \quad \text{for } x \in [0,1] \quad (2)$$

$$\alpha q(1,t) + \beta T(1,t) = f(t) \text{ for } t \in (0,\infty), \quad (3)$$

where T is the temperature, $q = \partial T/\partial n$ is the heat flux, n is the outward normal at the boundary of the slab, T_0 and f are prescribed functions and α and β are known constants which are not simultaneously zero. The general boundary condition (3) includes the particular cases of the Dirichlet condition for $\alpha = 0$ and the Neumann condition for $\beta = 0$. The thermal diffusivity is assumed constant and, for simplicity, taken to be unity. In addition, temperature readings are provided at an arbitrary space location $x = d \in [0,1]$, namely

$$T(x,t) = g(t) \text{ for } x = d, \quad t \in (0,\infty), \quad (4)$$

where g is a known function. Of course, the selection of the boundaries $x = 0$ and $x = 1$ as representing the unknown and known boundary conditions, respectively, is only a matter of convenience as they can be reversed without any change in the principle of the method of solution. Further, when $d = 0$ the equations (1)–(4) reduce to the direct problem.

Based on the formulation in equations (1)–(4) it is required to determine the temperature

$$T(0,t) = \phi_1(t) \quad \text{for } t \in (0,\infty) \quad (5)$$

and the heat flux

$$q(0,t) = \phi_2(t) \quad \text{for } t \in (0,\infty) \quad (6)$$

at the initial surface location $x = 0$. However, in practice only a finite time domain is analysed such that the time t in equations (5) and (6) can be assumed to be bounded between 0 and t_f, i.e. $t \in (0,t_f]$, where t_f is an arbitrary but specified final time of interest. Finally, the inverse problem (1)–(6) formulated for an arbitrary location $d \in (0,1]$ is similar to the formulation obtained by taking $d = 1$ and this special case will also be investigated. In order to discretize the above problem the BEM is employed.

3. THE BOUNDARY ELEMENT METHOD

The existence of a fundamental solution for the governing differential equation enables the problem to be reformulated in an integral representation. For the problem considered in Section 2, the one-dimensional space and time-dependent fundamental solution of the heat conduction equation (1) is of the form, see for example Brebbia *et al.* [22],

$$F(x,t;\xi,\tau) = \frac{1}{[4\pi(t-\tau)]^{1/2}} \exp\left[-\frac{(x-\xi)^2}{4(t-\tau)}\right] H(t-\tau), \quad (7)$$

where H is the Heaviside function, which is included in order to emphasize the fact that the fundamental solution is identically zero for $\tau > t$. The use of the fundamental solution (7) enables the partial differential equation (1) to be transformed into the following integral equation:

$$\begin{aligned} \eta(x)T(x,t) = &\int_0^t q(0,\tau)F(x,t;0,\tau)\,d\tau \\ &+ \int_0^t q(1,\tau)F(x,t;1,\tau)\,d\tau \\ &- \int_0^t T(0,\tau)F'(x,t;0,\tau)\,d\tau \\ &- \int_0^t T(1,\tau)F'(x,t;1,\tau)\,d\tau \\ &+ \int_0^1 T(y,0)F(x,t;y,0)\,dy \end{aligned}$$

$$(x,t) \in [0,1] \times (0,\infty), \quad (8)$$

where the prime denotes the differentiation with respect to the outward normal n and $\eta(x)$ is a coefficient function defined to be 1 if $x \in (0,1)$ and 0.5 if $x \in \{0,1\}$. For simplicity, in the formulation of the BEM applied in this study, constant boundary elements, i.e. the temperature and the heat flux are assumed constant over each element, are used when the integral equation (8) is discretized. Higher-order elements, such as linear or quadratic can be used but, in general, they are more appropriate for multi-dimensional spaces rather than the one-dimensional case considered in this study.

The time interval $[0,t_f]$ is divided into N elements on each boundary $x = 0$ and $x = 1$ and the space interval $[0,1]$ into N_0 elements. If one takes x on the boundary, at $x = 0$ and $x = 1$, and uses the initial condition (2) then the integral equation (8) becomes

$$\begin{aligned} \tfrac{1}{2}T(x,\tilde{t}_i) = &\sum_{j=1}^{i} \left(\int_{t_{j-1}}^{t_j} q(0,\tau)F(x,\tilde{t}_i;0,\tau)\,d\tau \right. \\ &\left. + \int_{t_{j-1}}^{t_j} q(1,\tau)F(x,\tilde{t}_i;1,\tau)\,d\tau \right) \\ &- \sum_{j=1}^{i} \left(\int_{t_{j-1}}^{t_j} T(0,\tau)F'(x,\tilde{t}_i;0,\tau)\,d\tau \right. \end{aligned}$$

$$+\int_{t_{j-1}}^{t_j} T(1,\tau)F'(x,\tilde{t}_i;1,\tau)\,d\tau\Bigg)$$
$$+\sum_{j=1}^{N_0}\int_{y_{j-1}}^{y_j} T_0(y)F(x,\tilde{t}_i;y,0)\,dy$$
$$i=\overline{1,N}, \quad (9)$$

where $x\in\{0,1\}$, t_{j-1} and t_j are the endpoints of an element and $\tilde{t}_j$ its midpoint. The boundary influence matrices are defined as

$$G_{ij}=\int_{t_{j-1}}^{t_j} F(x_i,\tilde{t}_i;\xi_j,\tau)\,d\tau \quad i,j=\overline{1,2N} \quad (10a)$$

$$E_{ij}=\int_{t_{j-1}}^{t_j} F'(x_i,\tilde{t}_i;\xi_j,\tau)\,d\tau+0.5\delta_{ij} \quad i,j=\overline{1,2N} \quad (10b)$$

$$F_{ij}=\int_{y_{j-1}}^{y_j} F(x_i,\tilde{t}_i;y,0)\,dy, \quad i=\overline{1,2N}, \quad j=\overline{1,N_0}, \quad (10c)$$

where δ_{ij} is the Kronecker delta symbol, $x_i=0$ for $i\leqslant N$, $x_i=1$ for $i>N$ and $\xi_j=0$ for $j\leqslant N$, $\xi_j=1$ for $j>N$ and we note that $G_{ij}=E_{ij}=0$ for $j>i$. With the notation (10), the integral equation (9) results in a system of linear algebraic equations and for constant elements has the form

$$\sum_{j=1}^{2N} G_{ij}q_j-\sum_{j=1}^{2N} E_{ij}T_j+\sum_{j=1}^{N_0} F_{ij}T_{0j}=0 \quad i=\overline{1,2N}, \quad (11)$$

where T_j,q_j are the values of the temperature T and the heat flux q at the node $\tilde{t}_j$, respectively, and T_{0j} takes the value of T_0 at the midpoint $\tilde{y}_j$ of the element $[y_{j-1},y_j]$.

As yet the discretized form of the boundary condition (3), namely

$$\alpha q_i+\beta T_i=f(\tilde{t}_i)=f_i \quad i=\overline{N+1,2N} \quad (12)$$

has not been utilized.

The system of equations (11) and (12) contains $3N$ equations and $4N$ unknowns, namely the temperature and the heat flux on the boundaries $x=0$ and $x=1$. In order to complete the system of equations, one must add further information represented by the internal measuremen's (4). The time interval $[0,t_f]$ on the space location $x=d$ is further discretized into N_T elements with $\tilde{t}'_i$ denoting the midpoint of the ith element on this interval. Applying the discretized form of equation (4) into the integral equation (8) results in

$$g_i=T(d,\tilde{t}'_i)=\sum_{j=1}^{i}\Bigg(\int_{t_{j-1}}^{t_j} q(0,\tau)F(d,\tilde{t}'_i;0,\tau)\,d\tau$$
$$+\int_{t_{j-1}}^{t_j} q(1,\tau)F(d,\tilde{t}'_i;1,\tau)\,d\tau\Bigg)$$
$$-\sum_{j=1}^{i}\Bigg(\int_{t_{j-1}}^{t_j} T(0,\tau)F'(d,\tilde{t}'_i;0,\tau)\,d\tau$$
$$+\int_{t_{j-1}}^{t_j} T(1,\tau)F'(d,\tilde{t}'_i;1,\tau)\,d\tau\Bigg)$$
$$+\sum_{j=1}^{N_0}\int_{y_{j-1}}^{y_j} T_0(y)F(d,\tilde{t}'_i;y,0)\,dy$$
$$i=\overline{1,N_T}. \quad (13)$$

For the special case $d=1$ the left hand side of equation (13) is multiplied by 0.5. Similarly with the definitions (10), one now introduces the following internal influences matrices:

$$GI_{ij}=\int_{t_{j-1}}^{t_j} F(d,\tilde{t}'_i;\xi_j,\tau)\,d\tau \quad i=\overline{1,N_T} \quad j=\overline{1,2N} \quad (14a)$$

$$EI_{ij}=\int_{t_{j-1}}^{t_j} F'(d,\tilde{t}'_i;\xi_j,\tau)\,d\tau \quad i=\overline{1,N_T} \quad j=\overline{1,2N} \quad (14b)$$

$$FI_{ij}=\int_{y_{j-1}}^{y_j} F(d,\tilde{t}'_i;y,0)\,dy \quad i=\overline{1,N_T} \quad j=\overline{1,N_0}, \quad (14c)$$

where $\xi_j=0$ for $j\leqslant N$ and $\xi_j=1$ for $j>N$, and we note that $GI_{ij}=EI_{ij}=0$ for $t_{j-1}>t'_i$. With the notation (14), the integral equation (13) results in another N_T linear equations, namely,

$$\sum_{j=1}^{2N} GI_{ij}q_j-\sum_{j=1}^{2N} EI_{ij}T_j+\sum_{j=1}^{N_0} FI_{ij}T_{0j}=g_i \quad i=\overline{1,N_T}. \quad (15)$$

All the integrals that occur in expressions (10) and (14) are numerically calculated, but it should be noted that singular causes do occur. However, for these singular integrals, which are typically of the form

$$I=\int_a^b F(x,t;\xi,\tau)\,d\tau \quad t\in[a,b] \quad (16a)$$

$$J=\int_a^b F'(x,t;\xi,\tau)\,d\tau \quad t\in[a,b] \quad (16b)$$

an analytical treatment can be implemented as follows. Taking into account the Heaviside function in relation (7) then expression (16a) becomes

$$I = \int_a^t \frac{1}{[4\pi(t-\tau)]^{1/2}} \exp\left[-\frac{(x-\xi)^2}{4(t-\tau)}\right] d\tau. \quad (17a)$$

By differentiating the function F, given by relation (7), with respect to the outward normal at ξ then expression (16b) becomes

$$J = -\int_a^t \frac{|x-\xi|}{[4\pi(t-\tau)]^{1/2}} \exp\left[-\frac{(x-\xi)^2}{4(t-\tau)}\right] d\tau. \quad (17b)$$

When $t = a$, $I = J = 0$, and when $x = \xi$, $I = ((t-a)/\pi)^{1/2}$ and $J = 0$, such that one may assume that $t \in (a,b]$ and $x \neq \xi$. Taking $\sigma = (t-\tau)^{-1/2}$ such that $d\tau = 2d\sigma/\sigma^3$, then this change of variable, together with some further calculations, results in expressions (17) becoming

$$I = C - \frac{|x-\xi|}{2} + \int_0^\delta \frac{(x-\xi)^2}{2\pi^{1/2}} \exp\left[-\frac{(x-\xi)^2\sigma^2}{4}\right] d\sigma \quad (18a)$$

$$J = -\tfrac{1}{2} + \int_0^\delta \frac{|x-\xi|}{2\pi^{1/2}} \exp\left[-\frac{(x-\xi)^2\sigma^2}{4}\right] d\sigma, \quad (18b)$$

where $\delta = (t-a)^{-1/2}$ and

$$C = \frac{1}{\delta\pi^{1/2}} \exp\left[-\frac{(x-\xi)^2\delta^2}{4}\right].$$

4. METHODS OF SOLUTION

At this stage one recalls that the application of BEM for the IHCP produced an algebraic system (11), (12) and (15) of $(3N+N_T)$ linear equations with $4N$ unknowns. In particular, equations (11) and (12) enable some of the unknowns, preferably the discretized temperatures T_j for $j = \overline{N+1,2N}$, i.e. on the boundary $x = 1$, and the heat fluxes q_j for $j = \overline{1,2N}$, i.e. on the boundaries $x = 0$ and $x = 1$, to be expressed as a function of the remaining discretized temperatures T_j for $j = \overline{1,N}$, i.e. on the boundary $x = 0$. Other choices of elimination of the variables, for example when only a Dirichlet condition is prescribed by equation (12) with $\alpha = 0$, will not introduce further complications. Without loss of generality, one may assume that $\alpha \neq 0$ and then the aforementioned elimination in equation (12) yields

$$q_i = \frac{f_i}{\alpha} - \frac{\beta T_i}{\alpha} \quad i = \overline{N+1,2N} \quad (19)$$

whilst the elimination of the heat flux in equation (11) yields

$$q_i = \sum_{j=1}^{2N} \sum_{l=1}^{2N} G_{ij}^{-1} E_{jl} T_l - \sum_{j=1}^{2N} \sum_{k=1}^{N_0} G_{ij}^{-1} F_{jk} T_{0k} \quad i = \overline{1,2N}. \quad (20)$$

Hence, expressions (19) and (20), when introduced into equations (15), lead to a lower order system of N_T linear equations with N unknowns, which in a generic form can be written in the form

$$\mathbf{AT} = \mathbf{b} \quad (21)$$

where $\mathbf{A} = (A_{ij})$ for $i = \overline{1,N_T}$, $j = \overline{1,N}$ is a matrix depending on the geometrical matrices introduced in expressions (10) and (14), $\mathbf{b} = (b_i)$ for $i = \overline{1,N_T}$ is a known vector and $\mathbf{T} = (T_j)$ for $j = \overline{1,N}$ is the unknown vector of the temperature on the boundary $x = 0$.

So far, the application of the BEM and boundary conditions (2)–(4) has reduced the IHCP to the linear system of algebraic equations (21). A necessary condition in order for a solution to be found is that $N_T \geqslant N$. Various methods can be considered for the solution of this system.

4.1. *Direct method*

Taking $N_T = N$, then the system of equations (21) contains N linear equations with N unknowns and, if the matrix $\mathbf{A}$ is invertible, one simply has

$$\mathbf{T} = \mathbf{A}^{-1}\mathbf{b}. \quad (22)$$

However, because the IHCP, equations (1)–(4), is improperly posed the system of equations (21) is ill-conditioned, and hence a direct solution, as given by equation (22), will be either impossible or will produce very inaccurate results.

4.2. *Least squares method*

Since the system of equations (21) is ill-conditioned, more information is necessary and this is achieved from the known data equation (4) taking $N_T > N$ such that the system becomes overdetermined. The number of interior measurements, N_T, should be chosen carefully so as not to be excessively large for the method to be of use in practical circumstances. However, at the same time N_T should not be too small because sufficient information is required for the uniqueness of the desired inverse problem. Using the least squares method, based on the minimization of the Euclidian norm $\|\mathbf{AT}-\mathbf{b}\|^2$ and solving a quadratic optimization problem, the solution of this system is given by, see for example Pasquetti and Le Niliot [23],

$$\mathbf{T} = (\mathbf{A}^{tr}\mathbf{A})^{-1}\mathbf{A}^{tr}\mathbf{b}, \quad (23)$$

where tr denotes the transpose of the matrix.

Results obtained from the application of the least-squares method are presented in Section 5. However, it has been found that this method produces oscillatory and inaccurate results, especially when noise is included into the data in order to simulate the error measured data.

4.3. *Regularization method*

To stabilize the results one may use smoothing constraints [14] and corresponding to the constraint that the function be continuous is the zeroth-order regularization, namely

$$\min\Lambda_0(\mathbf{T}) = \min\{\|\mathbf{AT}-\mathbf{b}\|^2+\lambda_0\|\mathbf{T}\|^2\} \quad (24a)$$

and corresponding to the constraint that the function be smooth is the first-order regularization, namely

$$\min\Lambda_1(\mathbf{T}) = \min\{\|\mathbf{AT}-\mathbf{b}\|^2+\lambda_1\|\partial\mathbf{T}/\partial x\|^2\}, \quad (24b)$$

where $\lambda_i \geqslant 0$, for $i = \overline{0,1}$ are the regularization parameters. The minimizations (24a) and (24b) are global and their solutions are given by

$$\mathbf{T}(\lambda_0) = (\mathbf{A}^{tr}\mathbf{A}+\lambda_0\mathbf{Id})^{-1}\mathbf{A}^{tr}\mathbf{b} \quad (25a)$$

$$\mathbf{T}(\lambda_1) = (\mathbf{A}^{tr}\mathbf{A}+\lambda_1\mathbf{R})^{-1}\mathbf{A}^{tr}\mathbf{b}, \quad (25b)$$

respectively, where **Id** is the identity matrix and the matrix $\mathbf{R} = (R_{ij})$ has the elements $R_{ii} = 1$ for $i = 1$ or $i = N$, $R_{ii} = 2$ for $i = \overline{2,(N-1)}$, $R_{i(i+1)} = -1$ for $i = \overline{1,(N-1)}$, $R_{i(i-1)} = -1$ for $i = \overline{2,N}$ and $R_{ij} = 0$ otherwise. From expressions (25) it can be seen that the solutions of the minimizations (24) depend on the regularization parameters λ_0 and λ_1 and their choice is crucial and difficult. When the regularization parameter is too large the numerical solution becomes smoother and may deviate substantially from the true solution, whilst when it is too small the numerical solution becomes oscillatory as happens in the limit $\lambda_0, \lambda_1 \to 0$, when the solutions (25) given by the regularization procedures become equal with the solution (23) given by the least squares method. However, for suitable values of the regularization parameters, which may be chosen according to the discrepancy principle [24]

$$\|\mathbf{AT}(\lambda)-\mathbf{b}\| = \|g(t)^{(\text{measured})}-g(t)^{(\text{exact})}\| \quad (26)$$

the regularization procedure produces stable results.

In order to eliminate the difficulty in choosing the regularization parameters, whilst maintaining the stability of the numerical solution, the minimal energy technique is employed.

4.4. *Minimal energy method*

In order to obtain a stable solution the exact internal condition (4) is replaced by the inequality

$$|T(d,t)-g(t)| \leqslant \varepsilon \text{ for } t\in(0,\infty), \quad (27)$$

where $\varepsilon \geqslant 0$ is a preassigned quantity, but this may introduce uniqueness problems due to enlarging the solution space. Using the discretized form of the inequality (27), instead of equation (15), and repeating the elimination of variables performed at the beginning of this section through the relations (19) and (20), a system of N_T linear constraints (double inequalities) with N unknowns is obtained, namely,

$$|\mathbf{AT}-\mathbf{b}| \leqslant \varepsilon \quad (28)$$

and some comments about the choice of ε will be presented at the end of this section.

For the steady case, the minimal energy method is based on a classical variational principle of the Laplace equation which involves the minimization of the kinetic energy functional

$$K(u) = \frac{1}{2}\iint_\Omega |\nabla u|^2\,dx\,dy. \quad (29)$$

Furthermore, based on Green's formula the relation (29) can be expressed in boundary integral form as

$$K(u) = \frac{1}{2}\int_{\partial\Omega} u\frac{\partial u}{\partial n}ds. \quad (30)$$

The minimization of the kinetic energy functional (29), subject to the constraints (28), was considered by Han [25] for the study of elliptic, improperly posed problem and further applications of this method were presented by Ingham *et al.* [17] and Ingham and Yuan [26] for the study of steady, linear and nonlinear heat conduction equations. Recently, Han *et al.* [13] presented a possible formulation of the method for the backward heat conduction problem and the purpose of this study is to extend this formulation to IHCP.

In the present investigation the minimization of the kinetic energy

$$KE(T) = \int_0^{t_f}\int_0^1 \left|\frac{\partial T(x,\tau)}{\partial x}\right|^2 dx\,d\tau \quad (31)$$

is analysed. For convenience and for a physical interpretation the energy equation is derived by multiplying the governing equation (1) by $T(x,t)$ and integrating over the domain $[0,1]\times[0,t_f]$. A further integration by parts enables the resulting equation to be written as

$$\int_0^{t_f} T(1,\tau)\frac{\partial T(1,\tau)}{\partial x}d\tau - \int_0^{t_f} T(0,\tau)\frac{\partial T(0,\tau)}{\partial x}d\tau - \int_0^{t_f}\int_0^1 \left|\frac{\partial T(x,\tau)}{\partial x}\right|^2 dx\,d\tau = \frac{1}{2}\int_0^1 T^2(x,t_f)\,dx - \frac{1}{2}\int_0^1 T^2(x,0)\,dx, \quad (32)$$

where the left hand side denotes the absorbed (or released) thermal energy through $x = 0$ and $x = 1$ and the kinetic energy $KE(T)$, whilst the right hand side denotes the inner energy of the system at times $t = 0$ and $t = t_f$. Introducing the identity (32) into relation (31) yields

$$KE(T) = \int_0^{t_f} T(0,\tau)q(0,\tau)\,d\tau + \int_0^{t_f} T(1,\tau)q(1,\tau)\,d\tau - \frac{1}{2}\int_0^1 T^2(x,t_f)\,dx + \frac{1}{2}\int_0^1 T^2(x,0)\,dx. \quad (33)$$

In the discretized form relation (33) becomes

$$KE(\mathbf{T}) = \sum_{j=1}^{2N} (t_j - t_{j-1})T_j q_j + \frac{1}{2}\sum_{j=1}^{N_0} (y_j - y_{j-1})(T_{0j}^2 - T^2(\tilde{y}_j,t_f)) \quad (34)$$

where, on using the integral equation (8),

$$T(\tilde{y}_i,t_f) = \sum_{j=1}^{N}\left(\int_{t_{j-1}}^{t_j} q(0,\tau)F(\tilde{y}_i,t_f;0,\tau)\,d\tau + \int_{t_{j-1}}^{t_j} q(1,\tau)F(\tilde{y}_i,t_f;1,\tau)\,d\tau\right) - \sum_{j=1}^{N}\left(\int_{t_{j-1}}^{t_j} T(0,\tau)F'(\tilde{y}_i,t_f;0,\tau)\,d\tau + \int_{t_{j-1}}^{t_j} T(1,\tau)F'(\tilde{y}_i,t_f;1,\tau)\,d\tau\right) + \sum_{j=1}^{N_0}\int_{y_{j-1}}^{y_j} T_0(y)F(\tilde{y}_i,t_f;y,0)\,dy \quad i = \overline{1,N_0}. \quad (35)$$

As in relations (14) one can define the internal influence matrices

$$GII_{ij} = \int_{t_{j-1}}^{t_j} F(\tilde{y}_i,t_f;\xi_j,\tau)\,d\tau \quad i = \overline{1,N_0} \quad j = \overline{1,2N} \quad (36a)$$

$$EII_{ij} = \int_{t_{j-1}}^{t_j} F'(\tilde{y}_i,t_f;\xi_j,\tau)\,d\tau \quad i = \overline{1,N_0} \quad j = \overline{1,2N} \quad (36b)$$

$$FII_{ij} = \int_{y_{j-1}}^{y_j} F(\tilde{y}_i,t_f;y,0)\,dy \quad i = \overline{1,N_0} \quad j = \overline{1,N_0}. \quad (36c)$$

These matrices are evaluated numerically with the only singularities occurring when $j \in \{N,2N\}$. With the notation (36), the integral equation (35) in discretized form results in

$$\sum_{j=1}^{2N} GII_{ij}q_j - \sum_{j=1}^{2N} EII_{ij}T_j + \sum_{j=1}^{N_0} FII_{ij}T_{0j} = T(\tilde{y}_i,t_f) \quad i = \overline{1,N_0}. \quad (37)$$

The process of elimination given by relations (19), (20) and (37) when introduced into expression (34) results in a quadratic form for the kinetic energy as a function of the unknowns temperatures $\mathbf{T} = (T_j)$ for $j = \overline{1,N}$. This can be written in the following generic form:

$$KE(\mathbf{T}) = \mathbf{T}^{tr}\mathbf{Q}\mathbf{T} + \mathbf{Q}_1^{tr}\mathbf{T} + Q_2, \quad (38)$$

where $\mathbf{Q} = (Q_{ij})$ for $i, j = \overline{1,N}$, $\mathbf{Q}_1 = (Q_{1i})$ for $i = \overline{1,N}$ and Q_2 are known matrix, vector and constant, respectively, depending on the geometry and the known boundary conditions (2) and (3). Quadratic forms of the type (38) may be also obtained when discretizing the zeroth and first-order regularization functionals Λ_0 and Λ_1 given by expressions (24). However, it should be noted that the smoothing constraint imposed by the minimization of the kinetic energy functional (31) is referred to the whole solution domain rather than only to the boundary as is in the minimization in expressions (24). Therefore, more information about the character of solution may be achieved. In addition, based on expression (33) it can be seen that the minimization of $KE(T)$ regularizes both the boundary temperatures and heat fluxes.

The minimal energy method now reduces to finding the temperatures vector $\mathbf{T}$ which minimizes the kinetic energy functional equation (38), subject to the linear constraints of the type equation (28). This problem is solved using the NAG routine E04UCF based on the minimization of an arbitrary smooth function subject to certain constraints which may include simple bounds of variables and both linear and nonlinear constraints [27].

Other functionals for which minimization has been investigated include

$$E_1(T) = \int_0^{t_f} T(0,\tau)q(0,\tau)\,d\tau + \int_0^{t_f} T(1,\tau)q(1,\tau)\,d\tau \quad (39a)$$

$$E_2(T) = \frac{1}{2}\int_0^1 T^2(x,t_f)\,dx - \frac{1}{2}\int_0^1 T^2(x,0)\,dx \quad (39b)$$

but it was found that these functionals produce poorer estimates of the analytical solutions compared with those obtained by minimizing the kinetic energy functional (31).

At this stage some comments about the method are appropriate. Although no regularization parameter is introduced explicitly, the numerical solution depends on the parameter ε through relations (28). It is well-known, see for example Brebbia *et al.* [22], that for the direct heat conduction problem, the BEM produces a stable and convergent solution, say $g_N(t) \to g(t)$. Therefore for a fixed number of meshes, N, in the case of error free data with $g(t)$ given by expression (4), the value of ε is taken as

$$\varepsilon = \varepsilon_0^N = \max\{|g_N(t) - g(t)| \, | \, t \in [0,t_f]\}. \quad (40)$$

Obviously from expression (40), ε is taken to be zero if, instead of condition (4) we enforce a 'direct problem solution' such as

$$T(d,t) = g_N(t), \quad t \in [0,t_f]. \tag{41}$$

As the number of elements, N, increases the value of ε_0^N given by expression (40) decreases and, in the most accurate case, might be taken equal with the machine precision, see also Philips [28]. For the case of error measured data which can be simulated by adding to the exact data, $g(t)$, a controlled small perturbation, $\tilde{g}(t)$, namely

$$T(d,t) = g(t) + \tilde{g}(t) \tag{42a}$$

or by adding random noisy data, ε_i, at each node on $x = d$, namely

$$T(d,\tilde{t}_i) = g_i + \varepsilon_i \quad i = \overline{1,N_T} \tag{42b}$$

the value of ε is taken as

$$\varepsilon = \varepsilon_0^N + \max\{|\tilde{g}(t)| \, t \in [0,t_f]\} \tag{43a}$$

and

$$\varepsilon = \varepsilon_0^N + \max\{|\varepsilon_i| i = \overline{1,N_T}\}, \tag{43b}$$

respectively. Further, in expressions (40) and (43) the L^2-norm instead of L^∞-norm may be employed, but then nonlinear constraints given by the L^2-norm, namely

$$\|\mathbf{AT} - \mathbf{b}\|^2 \leqslant \varepsilon^2 \tag{44}$$

should be imposed instead of the linear constraints (28). Although the estimations of ε given by expressions (40) and (43) seem to assume more *a priori* information about the exact data, $g(t)$, they only require the knowledge of the order of accuracy of the BEM employed when solving the direct heat conduction problem in the case of exact data and the tolerance of the measurements for noisy data. The smaller the value of ε that it is possible to choose, the better the numerical solution estimates the analytical solution. However, for too small values of ε no solution may exist for the minimization, equation (38), subject to the constraints, equation (28), and the routine used in this study gives an indication whether a feasible solution has been obtained or not under certain machine tolerances. Based on this discussion it seems that the choice of ε given by expressions (40) and (43), appears more natural and easier to implement than the choice of the regularization parameter, λ, given by expression (26).

5. NUMERICAL RESULTS AND DISCUSSION

The purpose of this section is to illustrate the applicability of the methods described in Section 4 for solving IHCP. As expected, the IHCP is ill-posed and therefore the direct method was found to be inapplicable since the discretized system of linear equation (21) is ill-conditioned.

The functions tested in this section are chosen in order to take into account the most difficult cases when the IHCP may not have a unique solution when the boundness of the solution is violated or when the boundary values are discontinuous [29].

Initially, the case of an unbounded solution is investigated by considering a simple smooth function,

$$T(x,t) = 2t + x^2 \tag{45}$$

as a test function which satisfies (1), together with a Robin boundary condition at $x = 1$ with $\alpha = \beta = 1$. Then the corresponding boundary conditions (2) and (3) become

$$T(x,0) = T_0(x) = x^2 \quad \text{for } x \in [0,1] \tag{46}$$

$$q(1,t) + T(1,t) = f(t) = 2t + 3 \quad \text{for } t \in (0,\infty) \tag{47}$$

and in the case of free error measurements the internal condition (4) is

$$T(d,t) = g(t) = 2t + d^2 \quad \text{for } t \in (0,\infty) \tag{48}$$

and initially the case $d = 1$ is considered.

In all the tables and the figures presented in this section the results for the surface temperature, $T(0,t)$, and the heat flux, $q(0,t)$, are shown at the nodes, $\tilde{t}_i$, for $i = \overline{1,N}$, on the boundary $x = 0$.

The effect of the choice of the value of t_f is illustrated by solving the problem in the domain $[0,1] \times [0,1]$ and in the domain $[0,1] \times [0,2]$ and the numerical results for the temperature and heat flux on the boundary $x = 0$ at some mesh points obtained with $N = N_0 = 40$ and $N_T = 80$ are shown in Tables 1 and 2. It should

Table 1a. Temperature on the boundary $x = 0$ for $t_f = 1$ when $d = 1$

t	No minimization	Least-squares	Minimal energy	Analytical solution
0.0125	0.12751	0.03493	0.03648	0.025
0.2125	1.25795	0.42596	0.42673	0.425
0.4125	0.07466	0.80297	0.81931	0.825
0.6125	0.91182	1.21483	1.22733	1.225
0.8125	11.4408	1.62454	1.61618	1.625
0.9875	2526.95	3100.43	2.03174	1.975

Table 1b. Heat flux on the boundary $x = 0$ for $t_f = 1$ when $d = 1$

t	No minimization	Least-squares	Minimal energy	Analytical solution
0.0125	0.81217	0.07837	0.09060	0.0
0.2125	11.6399	0.02096	0.00353	0.0
0.4125	−10.2086	−0.24720	−0.03358	0.0
0.6125	−1.70652	−0.20005	0.01105	0.0
0.8125	−3.77506	−0.00729	−0.06665	0.0
0.9875	20052.3	24566.0	−0.50749	0.0

Table 2a. Temperature on the boundary $x = 0$ for $t_f = 2$ when $d = 1$

t	No minimization	Least-squares	Minimal energy	Analytical solution
0.025	0.02828	0.04567	0.05705	0.05
0.425	0.76761	0.85009	0.85170	0.85
0.825	1.56224	1.64928	1.65203	1.65
1.225	2.46401	2.45128	2.45113	2.45
1.625	3.26365	3.25005	3.25162	3.25
1.975	44.3025	4.02155	3.92362	3.95

Table 2b. Heat flux on the boundary $x = 0$ for $t_f = 2$ when $d = 1$

t	No minimization	Least-squares	Minimal energy	Analytical solution
0.025	−0.12199	−0.02473	0.03926	0.0
0.425	−0.78696	0.00033	0.00089	0.0
0.825	−0.89397	−0.00633	0.00354	0.0
1.225	0.19995	0.01867	−0.00581	0.0
1.625	0.18773	0.00025	0.00065	0.0
1.975	228.856	0.40556	−0.55306	0.0

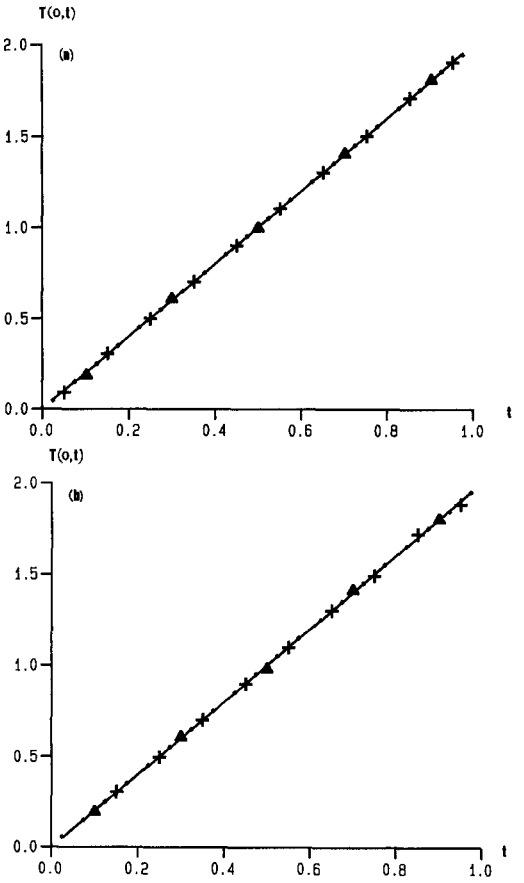

Fig. 1. The numerical results for the boundary temperature, $T(0,t)$, for the first test example in the case of the errorless data obtained using (a) the least-squares method, (b) the minimal energy method. The different mesh sizes used in the discretizations were (i) ▲ ▲ ▲ $N = 10$, $N_T = 20$, (ii) + + + $N = 20$, $N_T = 40$, (iii) ●●● $N = 40$, $N_T = 80$ and —— is the analytical solution.

be noted that the results for the surface temperature and heat flux on the specified boundary $x = 1$ were not included since in all the cases considered in this study they have been obtained with a relative error of less than 0.001%. Also, included in these tables are the numerical results obtained when no minimization is performed, and when only the linear constraints equation (28) are imposed. It can be seen that the method without minimization is inaccurate and is therefore not discussed further. From Tables 1a and 2a it can be seen that the numerical results for the temperature, using the least squares and the minimal energy methods, are very similar to the analytical solution up to a value of approximative 0.9 t_f. However, this conclusion is invalid for the heat flux when $t_f = 1$, see Table 1b, and this is due to the surface heat flux at time t being dependent on the interior values at times before and after t [16]. Also Tables 1 and 2 illustrate that the surface heat flux is more difficult to calculate accurately than are the surface temperatures. Therefore, the inaccurate values of the temperature near the end of the time interval $[0,t_f]$ will influence the accuracy of the surface heat flux over the whole time interval. Furthermore, in Table 1b the instability and oscillations in predicting the surface heat flux appear present when using the least squares method. This is probably because when using the least squares method the solution exhibits oscillatory behaviour and becomes unstable if a large number of unknowns are to be estimated (parameter estimation), whilst in the minimal energy the minimization of a functional reduces this effect. However, from Tables 2a and b, where $t_f = 2$, it can be observed that the results obtained using both numerical methods for the surface temperature and the heat flux are sufficiently close to the analytical solution for values of $t \leqslant t_f/2 = 1$. Hence, it is concluded that if $[0,t_f]$ is the time interval of interest then solving the problem on an extended interval gives rise to results which are in good agreement with the analytical solution on $[0,t_f]$, both for the boundary temperature and the heat flux.

In order to illustrate the rate of convergence of the least squares and the minimal energy methods, the numerical results are plotted in Figs. 1a, 2a and 1b, 2b, respectively, using three mesh sizes in the discretization, namely: (i) $N = 10$, $N_T = 20$; (ii) $N = 20$, $N_T = 40$; (iii) $N = 40$, $N_T = 80$. The value of N_0 was found not to significantly affect the results and throughout all the calculations the value of N_0 was taken to be 40. Also, in the numerical results presented in Figs. 1b and 2b the small control quantity ε was chosen to be $\mathbf{0}(10^{-3})$, which was found to be sufficiently small that any further decrease in this value did not produce any improvement in the agreement with the analytical solution and sufficiently large to ensure that the routine used gave a feasible solution.

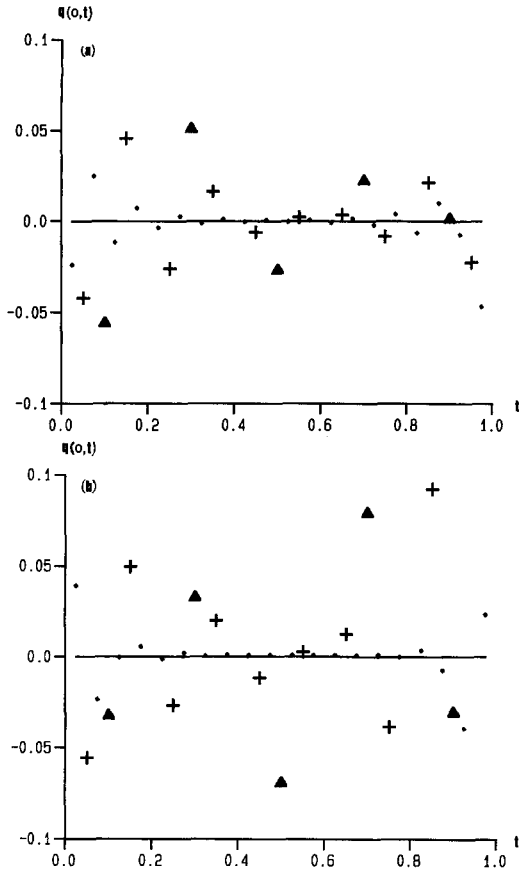

Fig. 2. The numerical results for the boundary heat flux, $q(0,t)$, for the first test example in the case of errorless data obtained using (a) the least-squares method, (b) the minimal energy method. The different mesh sizes used in the discretinizations were (i) ▲ ▲ ▲ $N = 10$, $N_T = 20$, (ii) + + + $N = 20$, $N_T = 40$, (iii) ●●● $N = 40$, $N_T = 80$ and —— is the analytical solution.

From Figs. 1 and 2 it is observed that the numerical solutions, as obtained both by using the least squares and the minimal energy methods, are in good agreement with the analytical solution and the accuracy in both numerical methods improves as the number of elements N on the space boundaries increase. Furthermore, using the three mesh sizes (i), (ii) and (iii) the values of the kinetic energy given by expression (38) for $t_f = 1$, were found to be 1.36876, 1.34615 and 1.33178, respectively, and these values appear to be converging to the analytical value of 4/3. Finally, from Figs. 1 and 2 it can be observed that the mesh size (iii) produces results which are closest to the analytical solution and therefore in order to illustrate further results the mesh size is fixed at $N = N_0 = 40$ and $N_T = 80$.

The effect of the value of $d \in [0,1]$ can be also examined from Table 3a where $d = 0.25$, Table 3b where $d = 0.5$ and Tables 1a, b where $d = 1$. Although the results obtained for the temperature and heat flux at $x = 0$ and with $t_f = 1$ appear to deteriorate as the distance d increases, and consequently increasing the domain in which the actual inverse problem is posed, when extending the time interval to $t_f = 2$ in exactly the same way as it has been explained for the results presented in Tables 2, it is possible to obtain a weak dependence of the results in the region of interest $[0,t_f]$ on the value of d as will be shown later in a comparison between Tables 2 and 4a. By taking the measurements closer to the surface where the unknowns are located, better agreement with the analytical solution is obtained but an optimal distribution of where the sensors should be located and where the time measurements should be taken remains a difficult problem [30], and will be investigated in another study. Finally, other types of boundary conditions, e.g. Dirichlet or Neumann have been tested and they were found to have very little effect on the accuracy of the results.

Since the IHCP is an improperly posed problem it is necessary to investigate the stability of the numerical schemes that one has employed. Therefore some errors are introduced into both the internal and the boundary data through a small perturbation function $\tilde{T}(x,t)$. Then the stabilility of the problem concerns how large an error will be generated by this perturbation in the solution. Thus, we consider

$$T_1(x,t) = T(x,t) + \tilde{T}(x,t), \tag{49}$$

where $T(x,t)$ is the original function given by the definition (45) and the perturbation function $\tilde{T}(x,t)$ is expressed as

$$\tilde{T}(x,t) = \chi(\gamma)\sqrt{2}\cos\left(2\gamma^2 t - \gamma x - \frac{\pi}{4}\right)\exp(-\gamma x), \tag{50}$$

where $\gamma = k^2\pi^2$, $\chi(\gamma) = 0$ if $k = 0$, $\chi(\gamma) = 1$ if $k \neq 0$ and k is a constant which has to be prescribed. Physically the perturbation function $\tilde{T}$ represents the quasi-stationary temperature distribution in a semi-infinite solid subject to a periodically varying heat flux at the boundary surface $x = 0$, see Özişik [31]. The perturbation $\tilde{T}$ satisfies the heat equation (1) and has the maximum amplitude

$$\tilde{T}_{max} = \chi(\gamma)\sqrt{2}\exp(-\gamma x). \tag{51}$$

Equation (51) shows that the maximum temperature in the interior region attenuates exponentially as the distance x from the surface increases. However, the inverse problem in which the surface temperature is to be determined through the use of the internal measurements, becomes sensitive to the errors in the input data which will be amplified exponentially with the distance x. It is clear from equation (51) that when γ is sufficiently large the maximum value of the amplitude $\tilde{T}_{max}$ is very small. Thus $\tilde{T}$ represents a small perturbation to the exact input data equations (46)–(48) which when perturbed become

Table 3a. Temperature and heat flux on the boundary $x = 0$ for $t_f = 1$ when $d = 0.25$

	Least-squares		Minimal energy		Analytical solution	
t	$T(0,t)$	$q(0,t)$	$T(0,t)$	$q(0,t)$	$T(0,t)$	$q(0,t)$
0.0125	0.02312	−0.01526	0.02374	−0.01039	0.025	0.0
0.2125	0.42492	−0.00005	0.42458	−0.00094	0.425	0.0
0.4125	0.82491	−0.00001	0.82453	0.00085	0.825	0.0
0.6125	1.22505	0.00065	1.22530	0.00334	1.225	0.0
0.8125	1.62514	0.00027	1.62535	0.00070	1.625	0.0
0.9875	1.97134	−0.03469	1.97412	−0.01108	1.975	0.0

Table 3b. Temperature and heat flux on the boundary $x = 0$ for $t_f = 1$ when $d = 0.5$

	Least-squares		Minimal energy		Analytical solution	
t	$T(0,t)$	$q(0,t)$	$T(0,t)$	$q(0,t)$	$T(0,t)$	$q(0,t)$
0.0125	0.019349	−0.04520	0.02419	−0.00650	0.025	0.0
0.2125	0.42505	−0.00025	0.42560	−0.00037	0.425	0.0
0.4125	0.82527	0.00281	0.82561	0.00149	0.825	0.0
0.6125	1.22502	0.00037	1.22544	0.00024	1.225	0.0
0.8125	1.62498	−0.00018	1.62555	0.00130	1.625	0.0
0.9875	2.00066	0.21742	1.93569	−0.41421	1.975	0.0

Table 4a. The temperature and heat flux on the boundary $x = 0$ for $t_f = 2$ when $d = 0.25$ and $k = 0$

	Least-squares		Minimal energy		Equation (49)	
$k = 0$						
t	$T(0,t)$	$q(0,t)$	$T(0,t)$	$q(0,t)$	$T_1(0,t)$	$q_1(0,t)$
0.025	0.04546	−0.02571	0.04447	−0.03124	0.05	0.0
0.225	0.44939	−0.00095	0.45043	0.01002	0.45	0.0
0.425	0.84953	0.00005	0.84999	0.00148	0.85	0.0
0.625	1.24970	0.00044	1.25081	0.00250	1.25	0.0
0.825	1.65017	0.00222	1.65161	0.00311	1.65	0.0
0.975	1.94096	−0.05749	1.93706	−0.09427	1.95	0.0

Table 4b. The temperature and heat flux on the boundary $x = 0$ for $t_f = 2$ when $d = 0.25$ and $k = 3$

	Least-squares		Minimal energy		Equation (49)	
$k = 3$						
t	$T(0,t)$	$q(0,t)$	$T(0,t)$	$q(0,t)$	$T_1(0,t)$	$q_1(0,t)$
0.025	0.04867	0.07802	0.04802	0.07436	−0.68732	41.7000
0.225	0.44950	0.00116	0.45039	0.01099	1.82897	150.358
0.425	0.84954	0.00025	0.84999	0.00162	0.70737	−137.647
0.625	1.24970	0.00052	1.25082	0.00258	−0.03796	−62.5226
0.825	1.65017	0.00227	1.65161	0.00316	2.61444	177.544
0.975	1.94096	−0.05745	1.93706	−0.09423	0.78387	−32.5121

$$T_1(x,0) = T_{10}(x) = T_0(x) + \tilde{T}_0(x) = x^2 + \tilde{T}_0(x) \tag{52a}$$

$$q_1(1,t) + T_1(1,t) = f_1(t) = f(t) + \tilde{f}(t) = 2t + 3 + \tilde{f}(t) \tag{52b}$$

$$T_1(d,t) = g_1(t) = g(t) + \tilde{g}(t) = 2t + d^2 + \tilde{g}(t), \tag{52c}$$

where $q_1 = \partial T_1/\partial n$ and

$$\tilde{T}_0(x) = \chi(\gamma)\sqrt{2}\cos\left(\gamma x + \frac{\pi}{4}\right)\exp(-\gamma x) \tag{53a}$$

$$\tilde{f}(t) = x(\gamma)[(1-2\gamma)\cos(2\alpha^2 t - \alpha) + \sin(2\alpha^2 t - \alpha)]\exp(-\gamma) \tag{53b}$$

$$\tilde{g}(t) = \chi(\gamma)\sqrt{2}\cos\left(2\gamma^2 t - \gamma d - \frac{\pi}{4}\right)\exp(-\gamma d). \tag{53c}$$

Clearly $\tilde{T}_0, \tilde{f}$ and $\tilde{g}$ can be made as small as one wishes by increasing the value of γ. However, at the surface $x = 0$

$$\tilde{T}(0,t) = \chi(\gamma)\sqrt{2}\cos\left(2\gamma^2 t - \frac{\pi}{4}\right) \tag{54a}$$

$$\frac{\partial \tilde{T}}{\partial x}(0,t) = -2\chi(\gamma)\cos(2\gamma^2 t) \tag{54b}$$

and these terms are of order of unity. Hence $\tilde{T} = T_1 - T$ is of the order of unity at $x = 0$, implying that the continuous dependence on the initial data is violated.

Tables 4a and 4b show the numerical results for the surface temperature and heat flux for various values of the time $t \in (0,1)$ obtained by solving the problem with $t_f = 2$ and for $k = 0$ and 3, respectively. The internal condition (52c) is imposed at $d = 0.25$. From these tables, corresponding to the perturbed and unperturbed solutions, it is found that the results for the surface temperature are almost identical, but they do differ from the perturbed solution (49). The values of the heat flux differ slightly but are still reasonably accurate, since they are different from the large values of the heat flux given by differentiating equation (49). Consequently, the least squares and the minimal energy methods are able to recognize the correct solution when a small amount of noise is included in the input data.

Figure 3a shows the numerical results for the surface temperature and the heat flux, respectively, obtained by using the numerical methods in comparison with the unperturbed solution (45) when a large noise is included into the data. This large noise is simulated by taking $\gamma = 2\pi^2$, i.e. $k = \sqrt{2}$, in expression (50) which defines the perturbation function $\tilde{T}$. The surface temperature appears accurate when using both of the numerical methods, see Fig. 3a, but Fig. 3b shows that some of the numerical results for the surface heat flux exhibit oscillatory behaviour and that they are inaccurate when using the least squares method. However, when using the minimal energy technique these large oscillations are alleviated, showing the stability introduced by this method.

A more realistic procedure of simulating error measurements consists in the introduction of some noise into the internal condition (4) at each node, $\tilde{t}_i$, see also expression (42b), namely

$$T(d,\tilde{t}_i) = \tilde{g}(\tilde{t}_i) = \tilde{g}_i = g_i + \varepsilon_i \quad i = \overline{1,N_T}, \tag{55}$$

where ε_i is a Gaussian random variable of mean zero and standard deviation σ which is taken to be some percentage, p, of the maximum absolute temperature at the location $x = d$, namely

$$\sigma = p \times \max\{|T(d,t)| \, | \, t \in [0,t_f]\}. \tag{56}$$

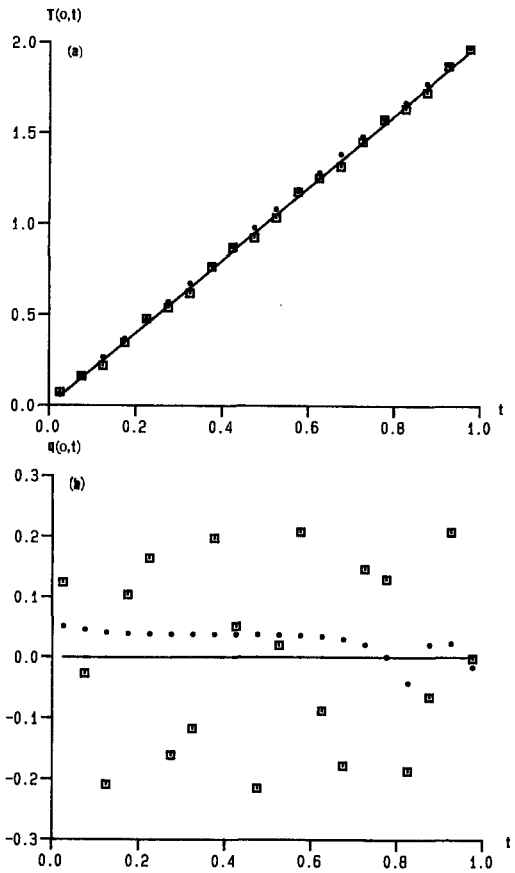

Fig. 3. A comparison between the results obtained using —— the analytical solution, □ □ □ the least squares method and ●●● the minimal energy method for (a) the boundary temperature, $T(0,t)$, and (b) the boundary heat flux, $q(0,t)$, for the case in which controlled errors given by expression (50) with $\gamma = 2\pi^2$ are included in the input data for the first test example.

The variables ε_i, for $i = \overline{1,N_T}$, are randomly generated by using the NAG routine G05DDF [32].

Figure 4 shows the exact data function, g, given by expression (48) and a $p\% = 5\%$ random noise

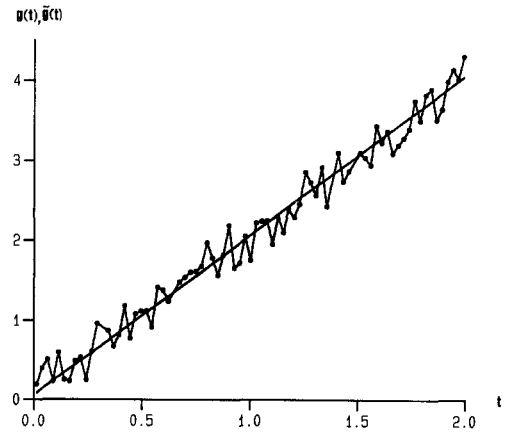

Fig. 4. The exact data function g (—) and a 5% random noise function $\tilde{g}$ (—●—) for the first test example.

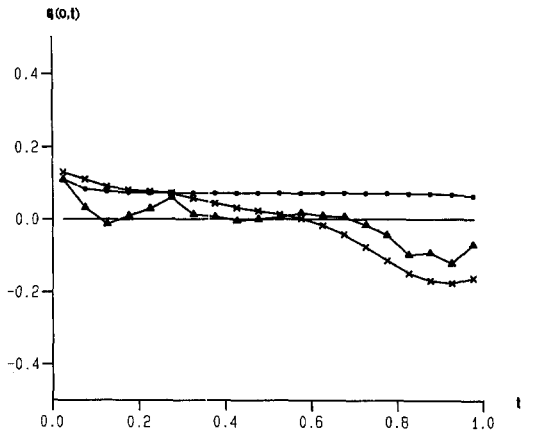

Fig. 5. The results for the boundary heat flux, $q(0,t)$, obtained using —— the analytical solution, ▲▲▲ the zeroth-order regularization procedure with $\lambda_0 = 0.5$, × × × the first-order regularization procedure with $\lambda_1 = 2$ and ●●● the minimal energy technique with $\varepsilon = 0.4$ for the case in which 5% noise is included into the measured data for the first test example.

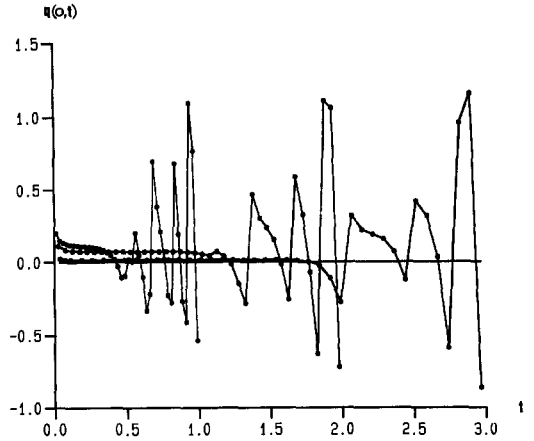

Fig. 6. A comparison of the results for the boundary heat flux, $q(0,t)$, obtained using —— the analytical solution and —●— the minimal energy technique for various time intervals $2t_f \in \{1, 2, 3\}$ with the corresponding values of $\varepsilon \in \{0.2, 0.4, 0.5\}$, respectively, for the case in which 5% noise is included into the measured data for the first test example.

function, $\tilde{g}$, given by expression (55) in the interval $[0,t_f(=2)]$ when $d = 0.25$. The function $\tilde{g}$ is introduced in order to simulate a typical set of error measured data which are likely to be recorded in the practical measurements of the temperature inside a heat conducting body.

Figure 5 presents the numerical results for the surface heat flux obtained using the minimal energy technique with $\varepsilon = 0.4$ taken according to relation (43b), the zeroth-order regularization with $\lambda_0 = 0.5$ and the first-order regularization with $\lambda_1 = 2$, for the simple test function given by expression (45) which satisfies a Neumann boundary condition (3) on $x = 1$, i.e. $\alpha = 1$ and $\beta = 0$, for a 5% noisy set of data shown in Fig. 4. The regularization method was chosen for comparison because it is a simple stable method which produces, in general, roughly the same good estimates as other stable methods, e.g. function specification, conjugate gradient, mollification, etc. Criteria for comparison of these stable methods can be found in Beck [33]. From the comparison with the analytical solution it is observed that both the regularization procedures and the minimal energy technique offer stable estimates and their L^2-error estimates defined by

$$\text{err} = \| q(0,t)^{(\text{calculated})} - q(0,t)^{(\text{analytical})} \| \qquad (57)$$

are 0.054, 0.097 and 0.074, respectively. The least squares numerical results are not presented herein since they produce an unstable solution, see Lesnic *et al.* [34]. It should be noted that in Fig. 5 the time interval of interest was taken to be $[0,t_f(=1)]$ although the problem was solved in the extended time interval $[0,2t_f(=2)]$.

Figure 6 shows the numerical results which have been obtained for the surface heat flux, $q(0,t)$, on the interval $t \in [0,2t_f]$ when using the minimal energy technique for various values of $t_f \in \{0.5, 1, 1.5\}$ with the corresponding parameters $\varepsilon \in \{0.2, 0.4, 0.5\}$, respectively, when 5% noise is included into the measured data. From this figure it is observed that up to the final time of interest t_f, the numerical results provide a good estimate of the analytical solution, and in the present work we have decided to ignore the numerical results on the remaining part of the time interval from t_f to $2t_f$. This effect is under further investigation as it probably depends on the unbounded behaviour of the test function chosen, the amount of noise included and/or the form of the functional to be minimized.

In the next example a more severe test function is taken, see Carslaw and Jaeger [35], namely

$$T(x,t) = \begin{cases} v(x,t), & t \in [0,0.5) \\ v(x,t) - 2v(x,t-0.5), & t \in [0.5,1) \\ v(x,t) - 2v(x,t-0.5) + 2v(x,t-1), & t \in [1,1.5) \\ v(x,t) - 2v(x,t-0.5) + 2v(x,t-1) & \\ \quad -2v(x,t-1.5), & t \in [1.5,2], \end{cases} \qquad (58)$$

where

$$v(x,t) = \frac{3(1-x)^2 - 1}{6} + t$$

$$-2\sum_{n=1}^{\infty} \frac{(-1)^n}{n^2\pi^2} \cos(n\pi(1-x)) \exp(-n^2\pi^2 t) \qquad (59)$$

which includes a discontinuous surface heat flux on $x = 0$.

Figure 7 illustrates the numerical results for the surface heat flux obtained using the minimal energy technique with $\varepsilon = 0.02$, the zeroth- and first-order regularization methods with $\lambda_0 = \lambda_1 = 0.01$, for the

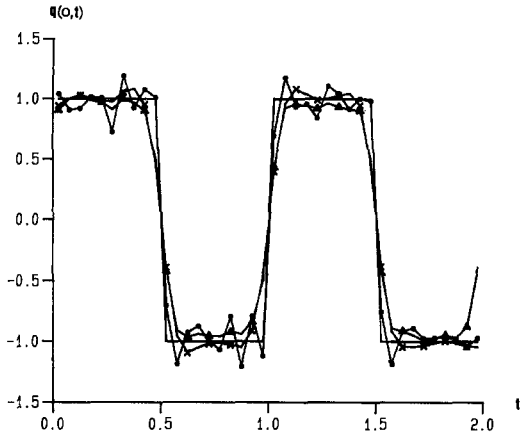

Fig. 7. The results for the boundary heat flux, $q(0,t)$, obtained using —— the analytical solution, ▲▲▲ the zeroth-order regularization procedure with $\lambda_0 = 0.01$, × × × the first-order regularization procedure with $\lambda_1 = 0.01$ and ●●● the minimal energy technique with $\varepsilon = 0.02$ for the case in which 5% noise is included into the measured data for the second test example.

test function given by expression (58) which satisfies a Neumann boundary condition (3) at $x = 1$, where there is 5% noise in the internal temperature measurements at the space location $d = 0.25$ during the time interval $[0,t_f(=2)]$. Due to the discontinuities of the heat flux at the corners of its square-wave representation by the step function in Fig. 7, inaccuracies of the numerical solution near these points are to be expected. As for the first test example the regularization procedures and the minimal energy technique produce stable approximate estimations for the analytical solution and their L^2-error estimates, defined by expression (57), are 0.338, 0.326 and 0.192, respectively.

Finally, extensions to nonlinear and higher dimensions inverse heat conduction problems of the numerical methods employed in this study can be easily accommodated.

6. CONCLUSIONS

In inverse heat conduction problems the unknown surface temperature and heat flux are associated with the boundary only, and in this study the discretization of the IHCP has been performed by using the BEM which has the advantage that no domain discretization is needed as requested when using finite differences or finite elements. Based on the BEM, the IHCP is reduced to solving an ill-conditioned linear system of algebraic equations and therefore, the direct method presented in Section 4.1 cannot be applied. This results in the nonuniqueness of the solution which may be overcome by increasing the number of equations. Two test examples are analysed in order to simulate the theoretical uniqueness problems given by the case of unbounded solutions or discontinuous boundary values. For exact data the least squares method presented in Section 4.2 gives good agreement with the analytical solutions for the surface temperature and heat flux provided that, in general, the known boundary condition is extended over a suitable additional time interval such that accurate results can be obtained over the complete earlier time domain. However, this method has been found unstable with respect to small perturbations in the input data and therefore the regularization procedure (zeroth- and first-order) has been introduced in Section 4.3. The regularization procedure modifies the least-squares method by adding an implicit order smoothing constraint for the boundary unknowns through the introduction of a regularization parameter. For a suitable choice of this parameter the regularization procedure produced a good stable estimation of the analytical solutions. However, this choice may not be an easy task in practical computations. In order to eliminate this problem, whilst maintaining the stability, the minimal energy technique based on the minimization of the kinetic energy functional subject to certain constraints has been introduced in Section 4.4. The minimization of the kinetic energy is physically realistic and imposes a stronger smoothing constraint for the whole domain solution. The linear constraints depend on a small positive quantity, ε, which can be chosen more naturally and easier than choosing the regularization parameter. The numerical results obtained using the minimal energy technique show a good stable estimation of the analytical solutions, provided that, in general, an extension of the time interval on which the boundary conditions are imposed is performed. Although the same good estimates are also achieved when using the regularization procedures, it is concluded that the minimal energy technique offers an easier, stable alternative of replacing the regularization parameter and, in addition, based on the minimization of the kinetic energy functional, the smoothing constraint is stronger since it is imposed for the whole domain solution. Furthermore, the extension of the BEM accompanied by the minimal energy technique to higher dimensions IHCP is straightforward.

REFERENCES

1. J. V. Beck, B. Blackwell and C. R. St Clair Jr, *Inverse Heat Conduction*. Wiley, New York (1985).
2. R. G. Hills, M. Raynaud and E. Hensel, Surface variance estimates using an adjoint formulation for a one-dimensional nonlinear inverse heat conduction technique, *Numer. Heat Transfer* **10**, 441–461 (1986).
3. J. Hadamard, *Lectures on the Cauchy Problem in Linear Partial Differential Equations*. Yale University Press, New Haven (1923).
4. O. R. Burggraf, An exact solution of the inverse problem in heat conduction theory and applications, *J. Heat Transfer* **86C**, 373–382.
5. D. Langford, New analytic solutions of the one-dimensional heat equation for temperature and heat flow rate both prescribed at the same fixed boundary (with applications to the phase change problem), *Q. Appl. Math.* **24**, 315–322 (1966).

6. D. M. France and T. Chiang, Analytic solutions to inverse heat conduction problems with periodicity, *J Heat Transfer* **102,** 579–581 (1980).
7. K. Kurpisz and A. J. Nowak, Applying BEM and the sensitivity coefficient concept to inverse heat conduction problems. In *Advanced Computational Methods in Heat Transfer* (Edited by C. A. Brebbia), pp. 309–321. Springer, New York (1990).
8. C. A. Brebbia, Applications of the boundary element method for heat transfer problems, *Proceedings of the Conference Modelisation et Simulation en Thermique*, Ensma, Poitiers, pp. 1–18 (1984).
9. C. Le Niliot, C. Papini and R. Pasquetti, Boundary element method for inverse heat conduction problems. In *Advanced Computational Methods in Heat Transfer* (Edited by C. A. Brebbia), pp. 285–295. Springer, New York (1990).
10. K. Kurpisz and A. J. Nowak, BEM approach to inverse heat conduction problems, *Engng Anal. Bound. Elem.* **10,** 291–297 (1992).
11. Y. Yuan, Application of the boundary element method to nonlinear and improperly posed problems. PhD Thesis, University of Leeds (1993).
12. D. B. Ingham and Y. Yuan, *The Boundary Element Method for Solving Improperly Posed Problems* (Edited by C. A. Brebbia and J. J. Connor), Vol. 19. Computational Mechanics, Southampton (1994).
13. H. Han, D. B. Ingham and Y. Yuan, The boundary-element method for the solution of the backward heat conduction equation, *J. Comput. Phys.* **116,** 292–299 (1995).
14. A. N. Tikhonov and V. Y. Arsenin, *Solutions of Ill-Posed Problems*. Winston-Wiley, WA (1977).
15. C. F. Weber, Analysis and solution of the ill-posed inverse heat conduction problem, *Int. J. Heat Mass Transfer* **24,** 1783–1792 (1981).
16. J. V. Beck, Nonlinear estimation applied to the nonlinear inverse heat conduction problem, *Int. J. Heat Mass Transfer* **13,** 703–716 (1970).
17. D. B. Ingham, Y. Yuan and H. Han, The boundary-element method for an improperly posed problem, *IMA J. Appl. Math* **47,** 61–79 (1991).
18. J. Skorek, Applying the least squares adjustment technique for solving inverse heat conduction problems, *Proceedings of the 8th Conference on Numerical Methods in Laminar and Turbulent Flow* (Edited by C. Taylor), pp. 189–198. Pineridge Press, Swansea (1993).
19. O. M. Alifanov, Solution of an inverse problem of heat conduction by iteration methods, *J. Engng Phys.* **26,** 682–687 (1974).
20. D. A. Murio, *The Mollification Method and the Numerical Solution of Ill-Posed Problems*. Wiley, New York (1993).
21. H. R. Busby and D. M. Trujillo, Numerical solution to a two-dimensional inverse heat conduction problem, *Int. J. Numer. Meth. Engng* **21,** 349–359 (1985).
22. C. A. Brebbia, J. C. F. Telles and L. C. Wrobel, *Boundary Element Techniques: Theory and Application in Engineering*. Springer, New York (1984).
23. R. Pasquetti and C. Le Niliot, Boundary element approach for inverse heat conduction problems: application to a bidimensional transient numerical experiment, *Numer. Heat Transfer* **20,** 169–189 (1991).
24. A. Morozov, On the solution of functional equations by the method of regularization, *Soviet Math. Dokl.* **7,** 414–417 (1966).
25. H. Han, The finite element method in a family of improperly posed problems, *Math. Comput.* **38,** 55–65 (1982).
26. D. B. Ingham and Y. Yuan, The solution of a nonlinear inverse problem in heat transfer, *IMA J. Appl. Math.* **50,** 113–132 (1993).
27. P. E. Gill, S. J. Hammarling, W. Murray, M. A. Saunders and M. H. Wright, User's guide for LSSOL (version 1.0). Report SOL 86-1, Stanford University (1986).
28. D. L. Philips, A technique for the numerical solution of certain integral equations of the first kind, *J. Assoc. Comput. Mach.* **9,** 84–97 (1962).
29. J. R. Cannon, *The One-Dimensional Heat Equation*. Addison-Wesley, MA (1984).
30. E. Hensel, *Inverse Theory and Applications for Engineers*. Prentice Hall, NJ (1991).
31. M. N. Özişik, *Boundary Value Problems of Heat Conduction*. Dover, New York (1989).
32. R. P. Brent, Algorithm **488,** *Commun. A.C.M.* pp. 704–706 (1974).
33. J. V. Beck, Criteria for comparison of methods of solution of the inverse heat conduction problem, *Nucl. Engng Des.* **53,** 11–22 (1979).
34. D. Lesnic, L. Elliott and D. B. Ingham, Boundary element method and minimal energy technique for the inverse heat conduction problem. In *Proceedings of the Second International Conference on Dynamic System Identification and Inverse Problems* (Edited by O. M. Alifaniov, V. V. Mickhailov and A. V. Nenarokomov), Vol. 1, pp. A4.1–A4.12. St Petersburg (1994).